

An Advanced Cellular Automaton Method with Interpolated Flux Scheme and its Application to Modeling of Gate Currents in Si MOSFETs

K. Fukuda, K. Nishi

VLSI R&D Center, Oki Electric Industry Co., Ltd.,
550-1, Higashiasakawa-cho, Hachioji-shi, Tokyo 193, Japan

Abstract

An improved cellular automaton(CA) method is proposed in which an interpolated flux concept is introduced to suppress a well-known artificial diffusion problem. The new method allows larger mesh sizes both in real and momentum space without losing numerical accuracy. Consequently, it becomes a practical modeling tool of non-linear carrier transport in semiconductor devices. In its application to Si MOSFETs, obtained results are extremely stable beyond the advanced weighted Monte Carlo method. Furthermore, making the best use of the stability, gate currents are studied in detail. 2 peaks of gate currents on gate bias, so-called drain avalanche hot carrier(DAHC) and channel hot electron(CHE), are well explained by thermionic emission and Fowler Nordheim(FN) tunneling of hot carriers respectively.

1. Introduction

Solving Boltzmann transport equation(BTE) by Monte Carlo method(MC), carrier distribution functions(DFs) which are essential information for hot carrier analysis of Si MOSFETs can be obtained. Because MC requires a huge amount of computer resources to get stable solutions, some new approaches to solve BTE based on a cellular automaton(CA) concept have been developed by several groups[1-4]. Although CA produces fairly stable solutions, CA still needs a significant calculation time because of a lot of data arising from full momentum mesh points on every real space mesh points. In this paper, a new CA method is proposed in which interpolated flux scheme has been introduced to reduce the number of meshes drastically by allowing much larger mesh sizes both in momentum space and real space. The efficiency of the present method is demonstrated through applications to gate currents analysis of Si MOSFETs.

2. Numerical and Physical Models

As other CA approaches[1-4], carrier momentum distribution functions are stored in numerical tables defined on each geometrical mesh points (fig.1). To keep numerical

accuracy, not logical type but real type data are used in these tables and updated by each time steps. Potential is also updated to be consistent to carrier distribution functions(fig.2). In these steps, flux is calculated assuming interpolated distribution functions between adjacent mesh points which suppress the artificial diffusion problem mentioned in ref.[4]. The suppression of the artificial diffusion is schematically explained in fig.3. Interpolation is adopted also to momentum space. By the interpolation of physical quantities between adjacent meshes, much larger mesh sizes can be used without losing accuracy, compared with the conventional method without interpolation.

As for physical models, followings are used.

- (1) Energy band considering the shape of high energy electron's density of states[5].
- (2) Phonons and impact ionization scatterings consistent with the band model[5, 6].
- (3) Brooks-Herring model of impurity scattering modified in high doping conditions[7].
- (4) Surface scattering model considering the universal mobility in inversion layers[8].
- (5) Gate currents of thermionic emission and of tunneling with WKB approximation[9].

2-dimensional impurity profiles of the process of coded gate length of $0.5\mu\text{m}$ and gate oxide thickness of 9nm are obtained from our process simulator OPUS[10].

3. Application Results

The present method is applied to Si n-MOSFETs where steep slopes of carrier concentration, highly doped source/drain and rare events such as impact ionization and gate injection will cause difficulties even to the advanced weighted Monte Carlo method. Drain, substrate and gate currents versus gate voltage(V_{GS}) characteristics for drain biases(V_{DS}) of 3,4 and 5 volts are shown in fig.4. It is remarkable that all these currents from subthreshold region to saturation region can be obtained in the same CPU time(3 hours for each on EWS of 200-Spec92fp) while MC needs more CPU time in low current conditions. This is because these current values are not averaged ones as in MC, but snapshots where obtained distribution functions contain no fluctuation. Distributions of carrier concentration, carrier temperature and generation rates are shown in fig.5-7 which are again stable snapshots of the $V_{DS} = 5V, V_{GS} = 2V$ case. The peak position of the generation rate is more drain side than the peak of the electron temperature which is a reasonable non-local effect. Back to fig.4, 2 peaks of gate currents can be observed (at $V_{GS} = 3$ and $V_{GS} = 5$ on $V_{DS} = 5$ for examples) which are conventionally explained as DAHC($V_{GS} = 3$) and CHE($V_{GS} = 5$). Distributions of gate injection along the channel both for 2 peaks are shown in fig.8 as $V_{GS} = 3$ in a) and $V_{GS} = 5$ in b), where solid lines represent thermionic emission current while dashed lines represent FN tunneling. Such FN tunneling is of hot electrons just below the barrier height of thermionic emission because they feel narrower tunneling distances of triangular potential than low energy electrons. In case b) with $V_{GS} = 5$, electrons beyond the barrier are less than in case a), but below the barrier, more tunneling is induced by the higher gate bias. As a conclusion, it is well explained that DAHC is attributed to thermionic emission and CHE to FN tunneling of hot electrons respectively.

References

- [1] T. Iizuka and M. Fukuma, *Solid-St. Electron.*, vol. 33, no. 1, pp. 27-34, 1990.
- [2] A. Das and M.S. Lundstrom, *Solid-St. Electron.*, vol. 33, no. 10, pp. 1299-1307, 1990.

- [3] M.G. Ancona, *Solid-St. Electron.*, vol. 33, no. 12, pp. 1633-1642, 1990.
- [4] K. Kometer, G. Zandler and P. Volg, *Phys. Rev. B*, vol. 46, no. 3, pp. 1382-1394, 1992.
- [5] R. Brunetti, C. Jacoboni, F. Venturi, E. Sangiorgi and B. Ricco, *Solid-St. Electron.*, vol. 32, no. 12, pp. 1663-1667, 1989.
- [6] R. Thoma, H.J. Peifer and W.L. Engl, W. Quade, R. Brunetti and C. Jacoboni, *J. Appl. Phys.*, vol. 69, no. 4, pp. 2300-2311, 1991.
- [7] K. Fukuda and K. Nishi, *IEICE Trans. Electron.*, vol. E78-C, no. 3, pp. 281-287, 1995.
- [8] E. Sangiorgi and M.R. Pinto, *IEEE Trans. Electron Devices*, vol. ED-39, no. 2, pp. 356-361, 1992.
- [9] C. Huang, T. Wang, C.N. Chen, M.C. Chang and J. Fu, *IEEE Trans. Electron Devices*, vol. ED-39, no. 11, pp. 2562-2568, 1992.
- [10] K. Nishi, K. Sakamoto, S. Kuroda, J. Ueda, T. Miyoshi, and S. Ushio, *IEEE Trans. Computer-Aided Design.*, vol. CAD-8, no. 1, pp. 23-32, 1989.

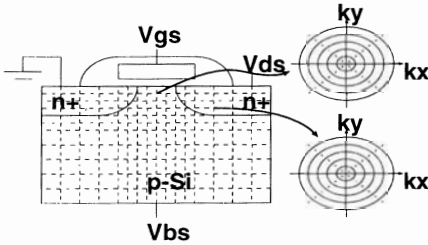


Figure 1: A schematic representation of momentum tables on each geometrical mesh points are shown. Each tables contain carrier distribution functions as real type data.

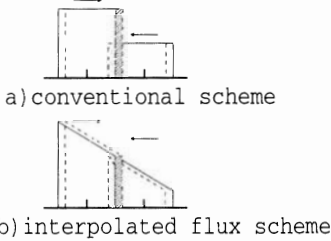


Figure 3: A schematic explanation of the suppression of artificial diffusion problem. In the conventional scheme a), flux is constant in assumed cells and the hatched boxes clearly show that flux is much more from the left cell to right. Such artificial diffusion is suppressed in the present method b).

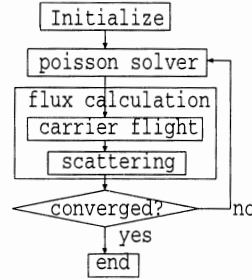


Figure 2: Flow chart of the presented simulation method. In the flux calculation, interpolated flux between adjacent mesh points is assumed.

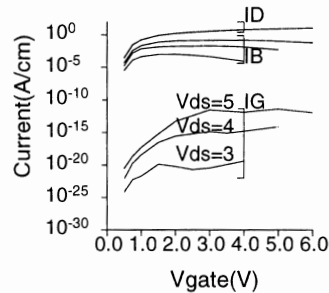


Figure 4: I_D, I_B and I_G versus V_{GS} on $V_{DS} = 3, 4$ and $5V$ which are stable over wide range.

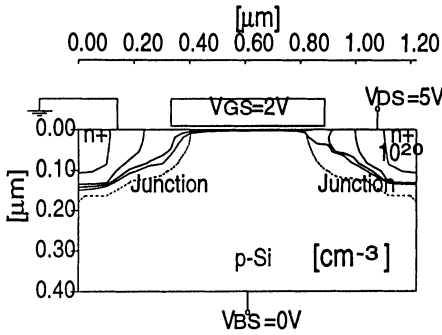


Figure 5: Carrier concentration of the $V_{DS} = 5$ and $V_{GS} = 2V$ case. Neighbouring lines differ by a factor of 10, referring to $10^{16}, \dots, 10^{20}(1/cm^3)$.

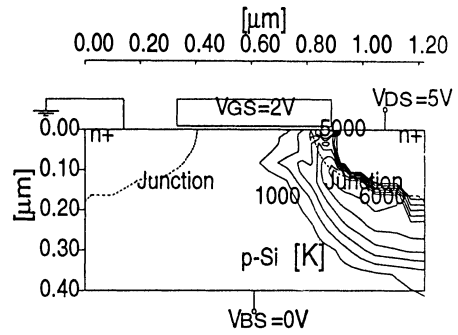


Figure 6: Carrier temperature of the same condition with fig.5. Neighbouring lines differ by 1000K, referring to 1000, ..., 6000K.

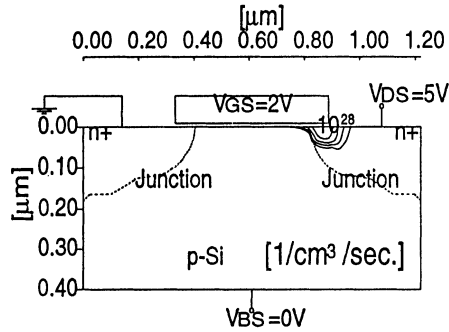


Figure 7: Generation rates of the same condition with fig.5. Neighbouring lines differ by a factor of 10, referring to $10^{25}, \dots, 10^{28}(1/cm^3/sec.)$.

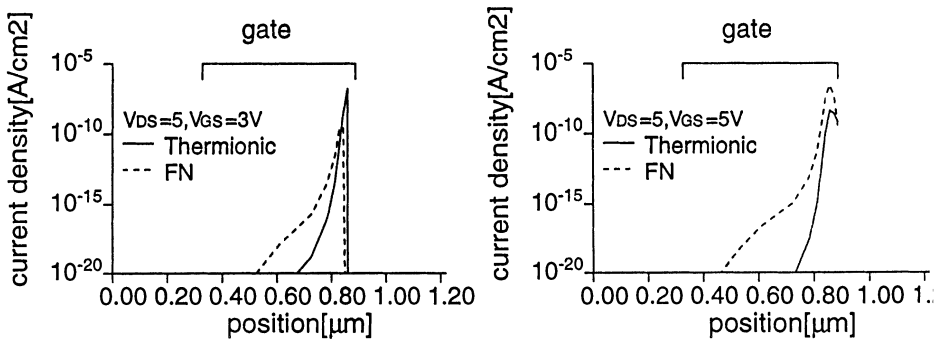


Figure 8: Carrier injection current density into SiO_2 along the channel for a) $V_{DS} = 5, V_{GS} = 3$ and b) $V_{DS} = 5, V_{GS} = 5V$ cases respectively where solid lines represent thermionic emission currents while dashed lines represent FN tunneling currents. In case b), FN tunneling of hot carriers dominates the gate current.